© EVS-25 Shenzhen, China, Nov. 5-9, 2010
The 25th World Battery, Hybrid and Fuel Cell Electric Vehicle Symposium & Exhibition

Contactless Power Transfer System for Electric Vehicle Battery Charger

Yuichi Nagatsuka[1], Shingo Noguchi[1], Yasuyoshi Kaneko[1], Shigeru Abe[1], Tomio Yasuda[2], Kazuhiko Ida[2], Akira Suzuki[3], and Ryoichi Yamanouchi[3]

[1]Saitama University, 255 Shimo-Okubo, Sakura-ku, Saitama-shi, Saitama 338-8570, Japan
[2]Technova Inc., 13th Fl. The Imperial Hotel Tower, 1-1 Uchisaiwai-cho 1-chome, Chiyoda-ku, Tokyo 100-0011, Japan
[3]Aisin AW Co., Ltd., 10 Takane, Fujii-cho, Anjo City, Aichi 444-1192, Japan

Abstract—A contactless power transfer system is desirable for the recharging of electric vehicles (EVs). Transformers with single-sided windings have been popular; however, transformers with double-sided windings are expected to be more compact and lightweight. A contactless power transfer system for EVs must have high efficiency, a large air gap, good tolerance to misalignment and be compact and lightweight. A novel transformer was developed using series and parallel capacitors with rectangular cores and double-sided windings to satisfy these criteria, and its characteristics are described. An output power of 1.5 kW and efficiency of 95% was achieved in the normal position. The characteristics of the system when a charge control circuit and lead acid batteries are connected to the secondary winding are also presented *Copyright Form of EVS25*.

Keywords— Contactless power transfer system, Efficiency, Electric vehicle, Plug-in hybrid vehicle, Battery charger

1. Introduction

The development and commercialization of plug-in hybrid electric vehicles (PHVs) and electric vehicles (EVs) is actively being realized, due to environmental concerns and rising oil prices. PHVs and EVs currently require connection to a power supply by electric cables for battery charging. A contactless power transfer system (such as that depicted in Figure 1) would have many advantages [1], including safety during high-power charging and the convenience of being cordless.

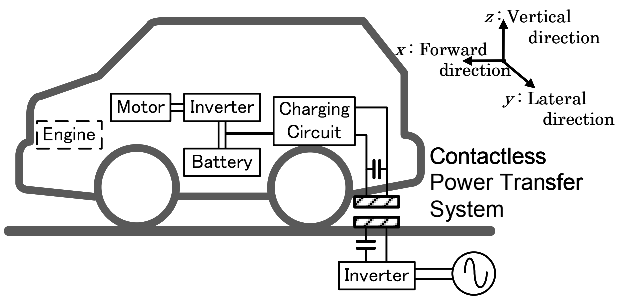

Figure 1: Schematic diagram of a contactless power transfer system for an electric vehicle.

The following specifications are very important for a contactless power transfer system for PHVs and EVs:

1. An efficiency of at least 95%.
2. An air gap of at least 70 mm.
3. Good tolerance to misalignment in the lateral direction (e.g., ±125 mm).
4. Compact and lightweight.

Because transformers have a large air gap, they have low coupling factors (0.1-0.5). Therefore, a high-frequency (10-50 kHz) inverter is used as the power supply in order to make the secondary voltage higher and resonant capacitors are connected to the terminals in order to compensate leakage reactance. Various resonant capacitor configurations have been proposed [2,3], of which a configuration where the primary capacitor is in series and the secondary capacitor is in parallel has an interesting characteristic [3]; if the capacitors are chosen correctly and the winding resistances are ignored, the equivalent circuit of a transformer with these capacitors is the same as an ideal transformer at the resonant frequency, which is equal to the inverter frequency.

Transformers with circular cores and single-sided windings have commonly been used [4,5]. However, we have revealed that a transformer with rectangular cores and double-sided winding has many advantages for the above specifications [4,6].

In this work, a novel 1.5 kW transformer with double-sided windings that has good tolerance to misalignment has been constructed for such a contactless system. The characteristics of the contactless power transfer system with a charging control circuit and batteries were investigated. The following sections describe the characteristics of the transformer and present various test results.

2. Contactless Power Transfer System for EVs

2.1 Contactless Power Transfer System

Figure 2 shows a schematic diagram of the contactless power transfer system with series and parallel resonant capacitors. A full-bridge inverter is used as a high-frequency power supply. The cores are made of ferrite and the windings are litz wires.

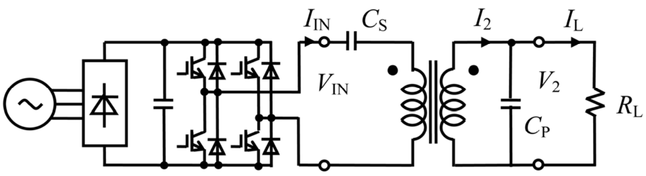

Figure 2: Contactless power transfer system.

New Energy and Industrial Technology Development Organization (NEDO) of Japan. *(Sponsor)*

2.2 Equivalent Circuit

Figure 3 shows a detailed equivalent circuit, which consists of a T-shaped equivalent circuit to which resonant capacitors C_S and C_P and a resistance load R_L have been added. Primary values are converted into secondary equivalent values using the turn ratio $a = N_1/N_2$ (primes are used to indicate converted values). As the winding resistances and the resistance of ferrite-core loss are much lower than the leakage and mutual reactances at the resonant frequency, the simplified equivalent circuit shown in Figure 4(a), which ignores the winding resistances (r'_1 and r_2) and the resistance of ferrite-core loss r'_0, is used.

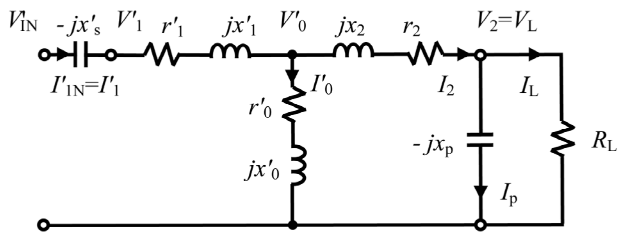

Figure 3: Detailed equivalent circuit.

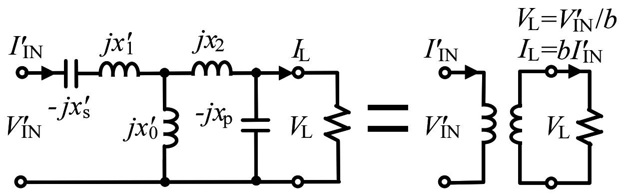

(a) Simplified equivalent circuit. (b) Ideal transformer.

Figure 4: Simplified equivalent circuit and ideal transformer.

2.3 Resonant Capacitors

To achieve resonance with the self-reactance of the secondary winding $\omega_0 L_2$, which is equivalent to adding a mutual reactance x'_0 and a leakage reactance x_2, the secondary parallel capacitor C_P is given by:

$$\frac{1}{\omega_0 C_P} = \omega_0 L_2 = x_p = x'_0 + x_2. \tag{1}$$

The primary series capacitor C_S (C'_S denotes its secondary equivalent) is determined as:

$$\frac{1}{\omega_0 C'_S} = x'_s = \frac{x'_0 x_2}{x'_0 + x_2} + x'_1. \tag{2}$$

2.4 Characteristics of an Ideal Transformer

V'_{IN} and I'_{IN} can be expressed as:

$$V'_{IN} = bV_2 = b\,V_L, \quad I'_{IN} = I_L/b, \quad b = \frac{x'_0}{x'_0 + x_2}. \tag{3}$$

Equation (3) represents the equivalent circuit of a transformer with these capacitors, which is the same as an ideal transformer with a turn ratio of b (Figure. 4(b)) at the resonant frequency.

2.5 Efficiency

The efficiency is approximated by:

$$\eta = \frac{R_L I_L^2}{R_L I_L^2 + r'_1 I'^2_1 + r_2 I_2^2} = \frac{R_L}{R_L + \dfrac{r'_1}{b^2} + r_2\left\{1 + \left(\dfrac{R_L}{x_P}\right)^2\right\}}. \tag{4}$$

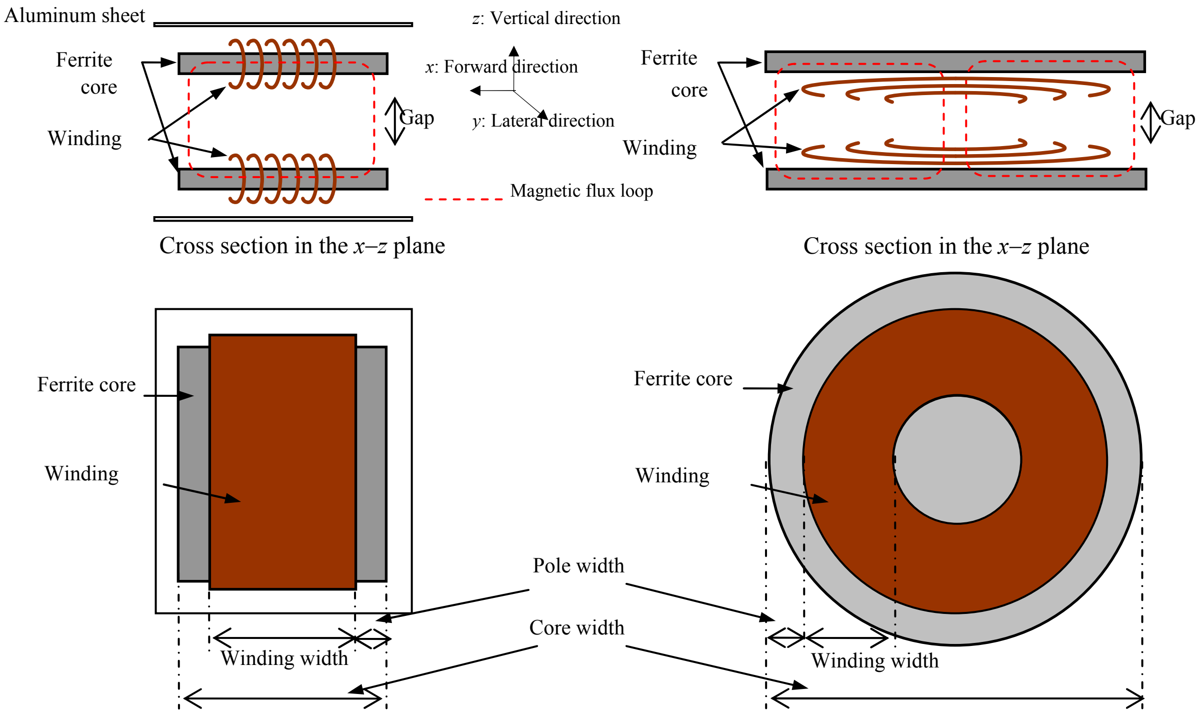

(a) Double-sided winding transformer (b) Single-sided winding transformer

Figure 5: Structures of single and double-sided winding transformers.

The maximum efficiency $\eta_{\max}$ is obtained when $R_L = R_{L\max}$:

$$R_{L\max} = x_p \sqrt{\frac{1}{b^2}\frac{r_1'}{r_2}+1} \quad \eta_{\max} = \frac{1}{1+\frac{2r_2}{x_p}\sqrt{\frac{1}{b^2}\frac{r_1'}{r_2}+1}} \quad (5)$$

If these characteristics are used, it is possible to design a transformer that has a maximum efficiency when the output power is equal to the rated power.

2.6 Comparison of Transformer Structure

Figure 5 shows a comparison of single- and double-sided winding transformer structures. The winding width must equal or exceed the gap length for the coupling factor to be greater than 0.2. The core width of the single-sided winding must be 2×(winding width + 2×pole width), whereas the core width of the double-sided winding need only be 1×(winding width + 2×pole width). Therefore, double-sided winding results in a transformer that can be made smaller than a single-sided winding transformer. Furthermore, the coupling factor of a single-sided winding transformer becomes zero when the horizontal misalignment is approximately half the core diameter [5].

However, double-sided winding transformers have a leakage flux at the back of the core, and consequently they have low coupling factors. To overcome this problem, an aluminum sheet is attached to the back of the core, as shown in Figure 5(a). The leakage flux is shielded by the aluminum sheet and the coupling factor becomes 50% larger than that without the aluminum sheet. The reduction in efficiency due to eddy current losses in the aluminum sheet is small (1-2%).

3. Characteristics of Double-Sided Winding Transformer

3.1 Specifications of the 1.5kW Transformer

A rectangular core and double-sided winding was used to provide the transformer with compactness and good tolerance to misalignment. Table 1 lists the specifications of a 1.5 kW double-sided winding transformer and Figure 6 shows a photograph of the transformer. The cores are made of ferrite and the windings are litz wires. A gap length of 70 mm with no misalignment is taken to be the normal position.

Table 1: Specifications of the 1.5 kW transformer.

Rated power		1.5 kW
Gap length		70±20 mm
Tolerance to Misalignment	Forward direction x	±45 mm
	Lateral direction y	±125 mm
Size		240×300×40 mm
Weight of the secondary transformer		4.6 kg

Figure 6: Photograph of the 1.5 kW transformer.

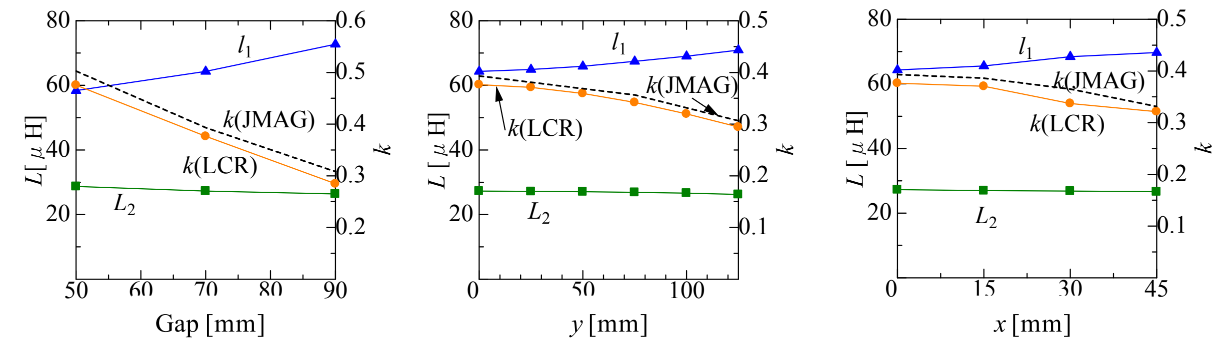

Figure 7: Transformer parameters.

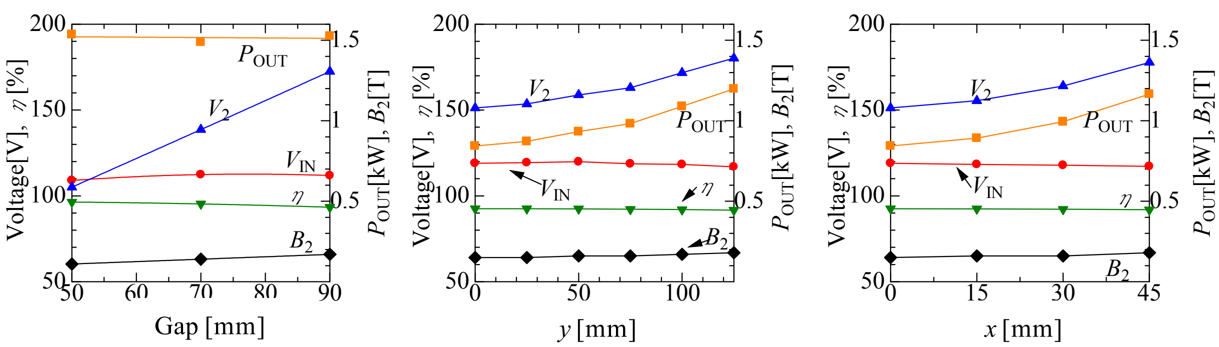

Figure 8: Transformer values.

Table 2: Experimental results.

Frequency [kHz]	20	
Gap length [mm]	70	140
k	0.376	0.158
b	0.369	0.154
R_L [Ω]	19.8	40.3
V_{IN} [V]	107	69.2
V_2 [V]	128	179
η [%]	95.3	89.5
B_1 [T]	0.11	0.18
B_2 [T]	0.13	0.18
C_S [μF]	0.696	0.654
C_P [μF]	2.30	2.44

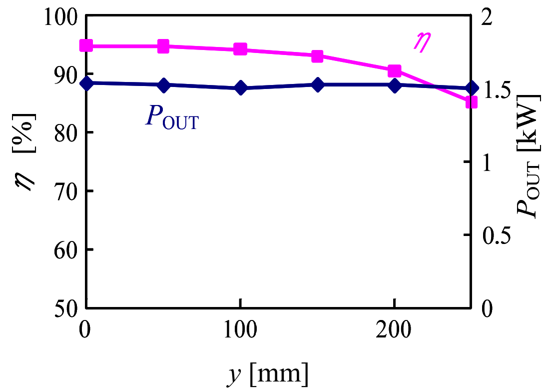

Figure 9: Characteristics of the 1.5 kW transformer with misalignment in the y direction.

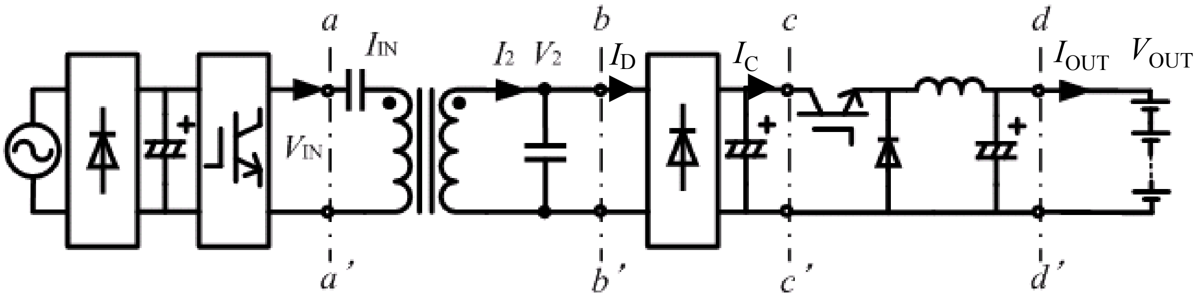

Figure 10: Contactless power transfer with charging system.

3.2 Experimental Results

3.2.1 Fundamental Characteristics

To investigate the fundamental characteristics of the 1.5 kW transformer, the power supply voltage (V_{AC} = 100 V) and the inverter frequency (f_0 = 20 kHz) were kept constant. The values of the resonant capacitors C_S and C_P for the normal position were kept constant. A full-bridge rectifier and resistance load were connected to the secondary winding.

Figure 7 shows the transformer parameters when the gap length or position is varied. In Figure 7, k (JMAG) shows the coupling factor calculated with JMAG, an electromagnetic field analysis software, and k (LCR) shows that calculated from inductances measured using an LCR meter. Figure 8 shows the transformer values for various gap lengths or positions. Figures 1 and 5 depict the misalignment directions.

From Figure 7, the coupling factor k decreased when the gap length or misalignment was increased, because the leakage flux became larger. The change in the value of the parallel capacitor C_P determined by Equation (1) was small, because the secondary self-inductance L_2 was almost constant. The coupling factor k and ideal transformer turn ratio b decreased when the gap length became larger, as shown in Figure 8; therefore, the secondary voltage V_2 and the output power P_{OUT} increased, as indicated by equation (3). The efficiency η was 95.3% at the normal position and 93.4% even at the highest gap length of 90 mm.

The voltage ratio (V_{IN}/V_2) changed when the position was varied and also when the gap length was changed. When the input voltage V_{IN} and the resistance load R_L were constant, the secondary voltage V_2 and the output power P_{OUT} increased when the misalignment increased. The efficiency was always greater than 91%, as shown in Figure 8. The results demonstrate that the rectangular double-sided winding transformer has good tolerance to misalignment.

3.2.2 Characteristics with a Wide Gap

The minimum ground clearance for PHVs and EVs is approximately 140 mm. The characteristics of the transformer with a wide gap are of particular interest with respect to practical application of the transformer for contactless power transfer. Table 2 shows the experimental results for the 1.5 kW transformer with gap lengths of 70 and 140 mm. Although the efficiency η decreased to 89.5%, it is possible to transfer 1.5 kW even at a gap length of 140 mm.

3.2.3 Characteristics with a Large Misalignment

One of the important features of the double-sided winding transformer is its characteristics with large misalignment of the lateral direction. The misalignment of the forward direction is easily limited by the use of wheel chocks, which help drivers to position the forward direction of the PHV/EV for charging.

The experimental results for a large misalignment of the lateral direction are shown in Figure 9. The efficiency was greater than 85% and the output power was 1.5 kW, even for a misalignment of 250 mm, which is equal to the core length. During the experiment, the input voltage V_{IN} was adjusted to maintain a constant secondary voltage V_2 and the values of the resonant capacitors Cs and Cp remained constant.

4. Charging System

4.1 Configuration of the Contactless Charging System

Figure 10 shows a schematic diagram of a contactless charging system. A charge control circuit, which consists of a full-bridge rectifier and chopper, was connected to the secondary winding. Constant current control is employed at the start of charging. If the charging voltage V_{OUT} reaches the transfer voltage, then the control is changed to constant voltage control.

4.2 Experimental Results

Six automotive lead acid batteries (12 V, 32 Ah) connected in series were used. The charging current was 4 A and the transfer voltage was 87 V for a charge time of 7 h. The batteries were discharged at 20 Ah from full charge. The experiment was started when the open circuit voltage of the lead acid batteries was 72 V.

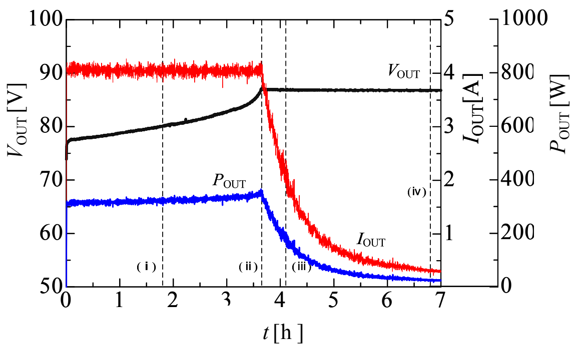

Figure 11: Characteristics of the charging system.

As shown in Figure 11, full charge of the batteries was successfully achieved and the estimated amount of charge was 18 Ah.

Figure 12 shows the waveforms of charging system at stages (i)-(iv) shown in Figure 11. The inverter output voltage V_{IN} and secondary voltage V_2 were constant, even if output power was varied. In addition, the inverter output voltage V_{IN} and current I_{IN}, and the secondary voltage V_2 were almost coherent. This demonstrates that the transformer with the charging system has the characteristics of an ideal transformer.

5. Conclusion

A contactless power transfer system is proposed that is suitable for application as an EV battery charger. A configuration with in series capacitors in the primary winding and in parallel capacitors in the secondary winding has an interesting characteristic, in that its equivalent circuit is the same as an ideal transformer. Consequently, the transformer has simple efficiency equations. A transformer consisting of rectangular cores with double-sided windings is compact and insensitive to misalignment in the lateral direction. A 1.5 kW transformer was constructed with dimensions of 240×300×40 mm, a gap length of 70±20 mm, a misalignment tolerance in the lateral direction of ±125 mm, a secondary winding and core mass of 4.6 kg, and efficiency of 95% in the normal position. Successful test results for a wide gap of 140 mm, for a large lateral misalignment of 250 mm and for lead acid battery charging were presented. In the future, we intend to impro-

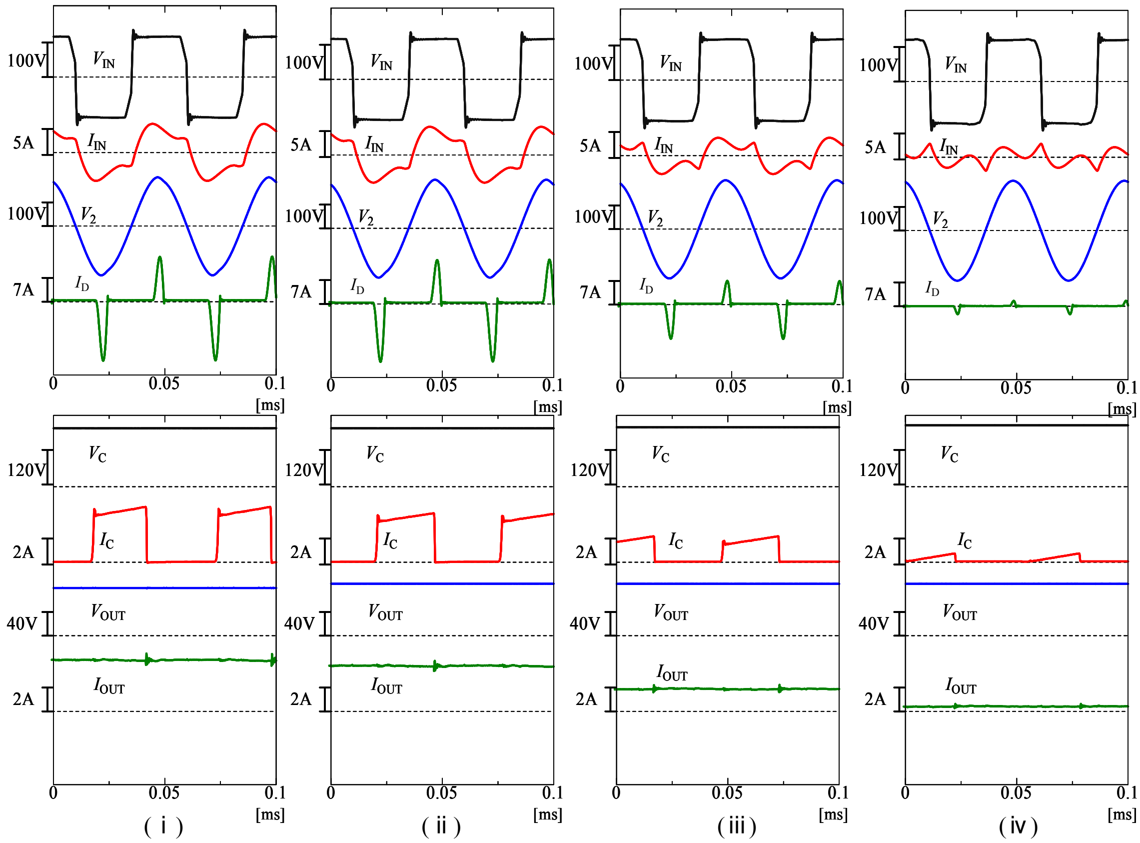

Figure 12: Waveforms of the charging system.

ve the design of the cores and windings to develop a transformer that is more lightweight and has higher efficiency.

This research was sponsored by the New Energy and Industrial Technology Development Organization (NEDO) of Japan.

6. References

[1] Y. Kamiya, Y. Daisho and H. Matsuki: "Inductive Power Supply System for Electric -driven Vehicles", IEEJ Journal, Vol. 128, No. 12, pp. 804-807 (2008) (in Japanese)

[2] A.W. Green and J.T. Boys: "10 kHz Inductively Coupled Power Transfer – Concept and Control", *IEE Power Electronics and Variable Speed Drives Conference*, *PEVD*, No. 399, pp. 694-699 (1994)

[3] T. Fujita, Y. Kaneko and S. Abe: "Contactless Power Transfer Systems using Series and Parallel Resonant Capacitors", IEEJ Trans. IA, Vol. 127, No. 2, pp. 174-180 (2007) (in Japanese)

[4] Y. Kaneko, N. Ehara, T. Iwata, S. Abe, T. Yasuda and K. Ida: "Comparison of Transformer Winding Methods for Contactless Power Transfer Systems of Electric Vehicle", IEEJ Trans. IA, Vol. 130, No. 6, pp. 734-741 (2010) (in Japanese)

[5] M. Budhia, G.A. Covic and J.T. Boys: "Design and Optimisation of Magnetic Structures for Lumped Inductive Power Transfer Systems", IEEE ECCE, pp. 2081-2088 (2009)

[6] Y. Nagatsuka, N. Ehara, Y. Kaneko, S. Abe and T. Yasuda: "Compact Contactless Power Transfer System for Electric Vehicles", IPEC2010-Sapporo, pp. 807-813 (2010)

7. Authors

Yuichi Nagatsuka
Saitama University
255 Shimo-Okubo, Sakura-ku, Saitama-shi, Saitama 338-8570, Japan
Tel:+81-48-858-3472 Fax:+81-48-858-0940
Email: s09mm222@mail.saitama-u.ac.jp
URL: http://akt.ees.saitama-u.ac.jp/

Shingo Noguchi
Saitama University
255 Shimo-Okubo, Sakura-ku, Saitama-shi, Saitama 338-8570, Japan
Tel:+81-48-858-3472 Fax:+81-48-858-0940
Email: s09mm226@mail.saitama-u.ac.jp
URL: http://akt.ees.saitama-u.ac.jp/

Yasuyoshi Kaneko
Saitama University
255 Shimo-Okubo, Sakura-ku, Saitama-shi, Saitama 338-8570, Japan
Tel:+81-48-858-3475 Fax:+81-48-858-3475
Email: kaneko@ees.saitama-u.ac.jp
URL: http://akt.ees.saitama-u.ac.jp/

Shigeru Abe
Saitama University
255 Shimo-Okubo, Sakura-ku, Saitama-shi, Saitama 338-8570, Japan
Tel:+81-48-858-9207 Fax:+81-48-858-9207
Email: abe@ees.saitama-u.ac.jp
URL: http://akt.ees.saitama-u.ac.jp/

Tomio Yasuda
Technova Inc.
13th Fl. The Imperial Hotel Tower, 1-1 Uchisaiwai-cho 1-chome, Chiyoda-ku, Tokyo 100-0011, Japan
Tel:+81-3-3508-2280 Fax:+81-3-3508-7578
Email: yasuda@technova.co.jp
URL: http://www.technova.co.jp

Kazuhiko Ida
Technova Inc.
13th Fl. The Imperial Hotel Tower, 1-1 Uchisaiwai-cho 1-chome, Chiyoda-ku, Tokyo 100-0011, Japan
Tel:+81-3-3508-2280 Fax:+81-3-3508-7578
Email: ida@technova.co.jp
URL: http://www.technova.co.jp

Akira Suzuki
AISIN AW CO., LTD. Product development planning department
10 Takane, Fujii-cho, Anjo City, Aichi 444-1192, Japan
Tel:+81-566-73-1616 Fax:+81-566-99-1433
Email: i12902_Suzuki@aisin-aw.co.jp
URL: http://www.aisin-aw.co.jp/

Ryoichi Yamanouchi
AISIN AW CO., LTD. Product development planning department
10 Takane, Fujii-cho, Anjo City, Aichi 444-1192, Japan
Tel:+81-566-73-1820 Fax:+81-566-99-1433
Email: i22269_Yamanouchi@aisin-aw.co.jp
URL: http://www.aisin-aw.co.jp/